

## A Derivation of fitness

To calculate fitness, we use the expected lifetime reproductive output,  $R_0$ . Generally, the expected lifetime reproductive output in an age-based model is the fecundity at age  $a$ ,  $m(a)$ , multiplied by the survivorship to age  $a$ ,  $l(a)$ , integrated over all ages:

$$R_0 = \int_0^{a_{max}} l(a)m(a)da. \quad (\text{A.1})$$

Using the growth function  $g(s) = ds/da$  to substitute size  $s$  for age simplifies the mathematics of describing  $R_0$  as a function of size at maturation and incorporating size-selective harvesting. In a size-based population, the expected lifetime reproductive output of an individual with size at maturation  $f$  in location  $x$  (in a protected or harvested area) is

$$R_0(x, f) = \int_{S_0}^{S_{max}} \frac{l(s, f, x)m(s, f)}{g(s, f)} ds, \quad (\text{A.2})$$

where  $S_0$  is the initial size and  $S_{max}$  is the asymptotic maximum size.

After maturation, the fecundity depends on size according to constants  $A$  and  $B$ ,

$$m(s, f) = \begin{cases} 0 & s < f \\ As^B & s \geq f \end{cases}, \quad (\text{A.3})$$

where  $A$  incorporates elevated levels of mortality during the pelagic larval stage; i.e.,  $m(s, f)$  represents the number of settling offspring before density-dependence. We base the fecundity parameters  $A$  and  $B$  on reported values of length-weight conversion and eggs produced per unit weight, with the proportion of eggs produced that become settling juveniles calibrated to produce realistic values of  $R_0$  (Table A.1).

The survivorship is

$$l(s, f, x) = \exp \left[ - \int_{S_0}^s \frac{u(S, x)}{g(S, f)} dS \right], \quad (\text{A.4})$$

| Species            | $A$                     | $B$   |
|--------------------|-------------------------|-------|
| Atlantic cod       | $3.6273 \times 10^{-6}$ | 3.0   |
| Bocaccio           | $3.7682 \times 10^{-6}$ | 3.061 |
| Yelloweye rockfish | $2.6563 \times 10^{-6}$ | 3.222 |
| Red snapper        | $2.6286 \times 10^{-6}$ | 2.953 |

Table A.1: Fecundity parameters for equation (A.3).  $A$  is the only calibrated parameter (see text), where  $B$  is from length-weight relationships; all other parameter values are available from the references cited in the Methods: Parameterization section.

where the mortality  $u(s, x)$  depends on natural mortality  $d$  and the size relative to minimum harvest size  $S_h$

$$u(s, x) = \begin{cases} d & s < S_h \\ d + h(x) & s \geq S_h \end{cases}, \quad (\text{A.5})$$

and the harvest mortality  $h(x)$  depends on the location

$$h(x) = \begin{cases} h_R & x \in \text{reserve} \\ h_H & x \notin \text{reserve} \end{cases}. \quad (\text{A.6})$$

In a slot fishery, with both a minimum harvest size  $S_h$  and a maximum harvest size  $S_m$ , the mortality is

$$u(s, x) = \begin{cases} d & s < S_h \\ d + h(x) & S_h \leq s \leq S_m \\ d + h_m(x) & s > S_m \end{cases}. \quad (\text{A.7})$$

Here, after the maximum size limit individuals experience catch-and-release mortality at a rate  $h_m(x) < h(x)$ .

Finally, if size  $s$  represents length, we assume individuals have a piecewise growth function, with a constant growth rate  $k_j$  before maturation and a slower, asymptotic growth rate toward maximum  $S_{max}$  at rate  $k_a$  after maturation:

$$g(s, f) = \begin{cases} k_j & s < f \\ k_a(S_{max} - s) & s \geq f \end{cases}. \quad (\text{A.8})$$

Roff (1983) bases an analogous discrete-time approach on the assumptions that (1) the observed decrease in growth after maturity is due to investment of resources in reproduction

rather than in growth and (2) the linear growth function observed in juveniles would continue in the absence of maturation (see also Heino and Kaitala 1997a,b; Perrin and Ruben 1990). Our growth parameters ( $S_{max}$ ,  $k_a$ , and  $k_j$ ) depend on the available von Bertalanffy growth parameters ( $L_\infty$  and  $k$ ) according to  $S_{max} = L_\infty$ ,  $k_a = k$ , and  $k_j = L_\infty(1/(1 - k) - 1)$ , analogous to Roff (1983).

Combining equations (A.2)-(A.8) indicates how size-at-maturation phenotype  $f$  and location in a protected or harvested area  $x$  determine the fitness  $R_0$  of an individual. This fitness definition uses a size-structured approach to derive fitness for a model without size structure. Underlying this approach is the simplifying assumption that size at maturation evolves slowly enough such that it is approximately constant across size classes within a given generation.

## Literature Cited

- Heino, M. and Kaitala, V. 1997a. Evolutionary consequences of density dependence on optimal maturity in animals with indeterminate growth. *Journal of Biological Systems* **5**:181–190.
- Heino, M. and Kaitala, V. 1997b. Should ecological factors affect the evolution of age at maturity in freshwater clams? *Evolutionary Ecology* **11**:67–81.
- Perrin, N. and Rubin, J. F. 1990. On dome-shaped norms of reaction for size-to-age at maturity in fishes. *Functional Ecology* **4**:53–57.
- Roff, D. A. 1983. An allocation model of growth and reproduction in fish. *Canadian Journal of Fisheries and Aquatic Sciences* **40**:1395–1404.

## B Calculation of size structure

Calculating the size structure of the population is necessary for the calculation of population growth rate and biomass yield. Under the assumption that the size-at-maturation distribution is approximately constant across size classes within generations and ignoring density dependence, the size-structured population dynamics follow the McKendrick-von Foerster equations

$$\frac{\partial n}{\partial t} + \frac{\partial}{\partial s} [\bar{g}(s)n(s, t)] = -u(s, x)n(s, t) \quad (\text{B.1})$$

$$\bar{g}(S_0)n(S_0, t) = \int_{S_0}^{S_a} \bar{m}(s)n(s, t)dw, \quad (\text{B.2})$$

where

$$\bar{g}(s) = \iint \hat{\psi}(f, g)g(s, f)dg df \quad (\text{B.3})$$

$$\bar{m}(s) = \iint \hat{\psi}(f, g)m(s, f)dg df \quad (\text{B.4})$$

and  $n(s, t)$  is the number of individuals of size  $s$  at time  $t$  (therefore,  $N(t) = \int n(s, t)ds$ ),  $\hat{\psi}(f, g)$  is the (approximately constant) phenotype-genotype distribution, and  $m(s, f)$ ,  $u(s, x)$ , and  $g(s, f)$  are defined in equations (A.3), (A.5), and (A.8).

The steady-state solution to equations (B.1)-(B.2) yields the equilibrium proportion of individuals of each size  $s$ ,  $\hat{\eta}(s)$  (VanSickle 1977):

$$\hat{\eta}(s, x) = \frac{\frac{\bar{l}(s, x)}{\bar{g}(s)} \exp \left[ - \int_{S_0}^s \frac{r}{\bar{g}(S)} dS \right]}{\int \frac{\bar{l}(s, x)}{\bar{g}(s)} \exp \left[ - \int_{S_0}^s \frac{r}{\bar{g}(S)} dS \right] ds}, \quad (\text{B.5})$$

where

$$\bar{l}(s, x) = \exp \left[ - \int_{S_0}^s \frac{u(S, x)}{\bar{g}(S)} dS \right] \quad (\text{B.6})$$

and  $r$  is the solution to the Euler-Lotka equation

$$1 = \int_{S_0}^{S_a} \frac{\bar{l}(s, x)\bar{m}(s)}{\bar{g}(s)} \exp \left[ - \int_{S_0}^s \frac{r}{\bar{g}(S)} dS \right] ds. \quad (\text{B.7})$$

Evaluating equation (B.7) for a particular  $\psi(t, f, g)$  gives the population growth rate  $r(\psi)$  for equation (6), and evaluating equation (B.5) when equations (5)-(6) reach an equilibrium gives the size structure for calculating equilibrium biomass yield.

## Literature Cited

Vansickle, J. 1977. Analysis of a distributed-parameter population model based on physiological age. *Journal of Theoretical Biology* **64**:571–586.

## C Details and results for the individual-based model

In forming the population-based model, we assume that  $R_0$  provides a measure of fitness, we ignore density-dependent growth, and we assume that evolutionary dynamics and changes in size structure occur on different time scales; the individual-based simulation provides a test of how important these assumptions are to the model outcome. This simulation starts with a population where each individual has a size, size-at-maturation genotype, size-at-maturation phenotype.

In each time step, mating repeatedly occurs between two individuals chosen at random. The number of offspring from each mating pair depends on their mean fecundities, determined by their sizes and size-at-maturation phenotypes as in equation (A.3). To match equation (3), each offspring inherits a size-at-maturation genotype based on its parental genotypes and the genetic variance in the population (random variable from a normal distribution with a mean of the average parental genotype and a variance of half the genetic variance plus mutation); its size-at-maturation phenotype depends on its genotype and the environment (random variable from a normal distribution with a mean of the the degree of plasticity times the optimum phenotype plus the remainder times the genotype and a variance of the environmental variance).

After reproduction, each individual in the population grows an increment dependent on its current size and its size-at-maturation phenotype, as in equation (A.8). To test the effect of density-dependent growth, an alternate version of the simulation reduces the growth rate by a factor of  $(1 + N/K)$ , analogous to Heino and Kaitala (1997). Finally, mortality occurs where the probability of each individual surviving in the time step depends on its initial and final size in the time step, the natural mortality, the harvest mortality, and the harvest size limit(s), as in equations (A.5)-(A.6). The simulation models reduced larval survivorship due to competition for space at settlement by multiplying the survivorship probability for new offspring by  $(1 - N/K)$ .

Within the individual-based model, population dynamics differ with the inclusion of

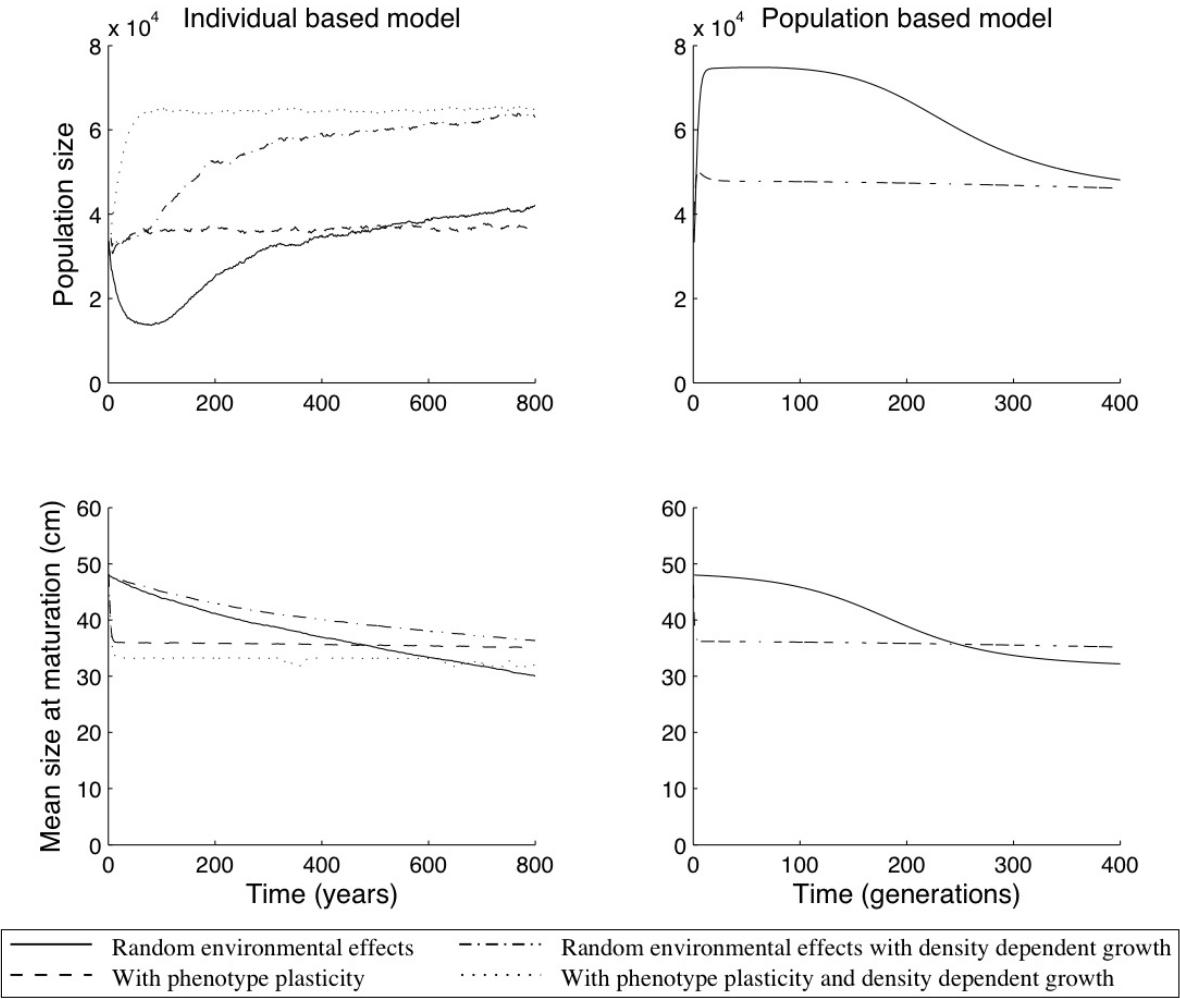


Figure C.1: Time trajectories for population size and size at maturation for bocaccio using the population and individual based models and the random environmental effects ( $\rho_f = 0$ ) and intermediate phenotype plasticity ( $\rho_f = 1 - h^2$ ) approaches, with a harvest mortality of 0.2 and minimum size limit of 48 cm.

density-dependent growth, while the trajectories for size-at-maturation evolution with and without density-dependent growth are more similar (Figure C.1). While the individual-based and population-based models follow different time trajectories for the random environmental effects approach, the trajectories for the intermediate phenotype plasticity approach and the equilibrium predictions for both approaches are similar (Figure C.1). These results support our treatment of density dependence, use of  $R_0$  as a measure of fitness, and separation of time scales for size structure changes and size-at-maturation evolution.

## Literature Cited

Heino, M. and Kaitala, V. 1997. Evolutionary consequences of density dependence on optimal maturity in animals with indeterminate growth. *Journal of Biological Systems* **5**:181–190.

## D Details and results for the spatially explicit model

To test the importance of assuming uniform density within individual protected or harvested areas when calculating the exchange rates in the two-pool model, we use a spatially explicit model. In the spatially explicit model, individuals disperse along a linear coast according to reaction-diffusion dynamics, where (analogous to the spatially implicit model) the diffusion term  $\sigma$  models random movement (Figure 2);  $\sigma$  is a measure of the average distance between parent and offspring that incorporates both planktonic larval dispersal and adult movement (Kirkpatrick and Barton 1997).

To derive a spatially explicit version of equations (8)-(11), let  $\phi(t, x, f, g)$  represent the total number of individuals at time  $t$  and location  $x$  with size-at-maturation phenotype-genotype combination  $(f, g)$ . Then individuals disperse along the coast according to

$$\frac{\partial \phi}{\partial t} = \frac{\sigma^2}{2} \frac{\partial^2 \phi}{\partial x^2}. \quad (\text{D.1})$$

Using the relationship that the total number of individuals is  $N(x, t) = \iint \phi(x, t, f, g) df dg$ , the spatial population dynamics are

$$\frac{\partial N}{\partial t} = \frac{\sigma^2}{2} \frac{\partial^2 N}{\partial x^2}. \quad (\text{D.2})$$

Similarly, using the relationship that the proportion of individuals with a phenotype-genotype combination is  $\psi(x, t, f, g) = \phi(x, t, f, g)/N(x, t)$ , the spatial genetic dynamics are

$$\frac{\partial \psi}{\partial t} = \frac{\sigma^2}{2} \frac{\partial^2 \psi}{\partial x^2} + \sigma^2 \frac{\partial \psi}{\partial x} \frac{\partial \ln(N)}{\partial x}. \quad (\text{D.3})$$

In the above equation, the  $\sigma^2 \frac{\partial \psi}{\partial x} \frac{\partial \ln(N)}{\partial x}$  term arises from asymmetric gene flow due to variable population size in space (Kirkpatrick and Barton 1997). Combining the spatial dynamics in equations (D.2)-(D.3) with the population and genetic dynamics in equations (5)-(6) yields (Barton 1999, Kirkpatrick and Barton 1997):

$$\frac{\partial N}{\partial t} = \frac{\sigma^2}{2} \frac{\partial^2 N}{\partial x^2} + r(x, \psi)N \left(1 - \frac{N}{K}\right) \quad (\text{D.4})$$

$$\frac{\partial \psi}{\partial t} = \frac{\sigma^2}{2} \frac{\partial^2 \psi}{\partial x^2} + \sigma^2 \frac{\partial \psi}{\partial x} \frac{\partial \ln(N)}{\partial x} - \psi + \quad (\text{D.5})$$

$$\mathcal{G}(f, (1 - \rho_f)g + \rho_f \nu_f(x), E) \iint \psi^*(g_1) \psi^*(g_2) \mathcal{G}\left(g, \frac{g_1 + g_2}{2}, G/2 + M\right) dg_1 dg_2,$$

where

$$\psi^*(x, t, g) = \frac{\int R_0(x, f)\psi(x, t, f, g)df}{\iint R_0(x, f)\psi(x, t, f, g)df dg} \quad (\text{D.6})$$

and the location  $x$  determines  $R_0(x, f)$  (equation (A.2)),  $r(x, \psi)$  (equation (B.7)), and  $\nu_f(x)$  by dictating the harvest mortality, a step function of  $x$ .

The spatially explicit reaction-diffusion model (equations (D.4)-(D.6)) and spatially implicit two-pool model (equations (8)-(13)) yield quantitatively different population trajectories, though with similar relative population size in protected and harvested areas, and similar size-at-maturation trajectories (Figure D.1). To determine whether the spatially explicit and implicit models yield different equilibrium predictions with varying MPA network designs and traditional fisheries management limits, we compare the models with parameters long-distance dispersal and strong selection, because they have the greatest exchange rates and the greatest difference in selection pressure between protected and harvested areas and therefore are most likely to be affected by the assumptions made in forming the spatially implicit model. The qualitatively similar results from the two models (Figure D.2) verifies the robustness of qualitative predictions from our model to the assumption of even density within each subarea.

## Literature Cited

Barton, N. H. 1999. Clines in polygenic traits. *Genetical Research* **74**:223–236.

Kirkpatrick, M. and Barton, N. H. 1997. Evolution of a species' range. *American Naturalist* **150**:1–23.

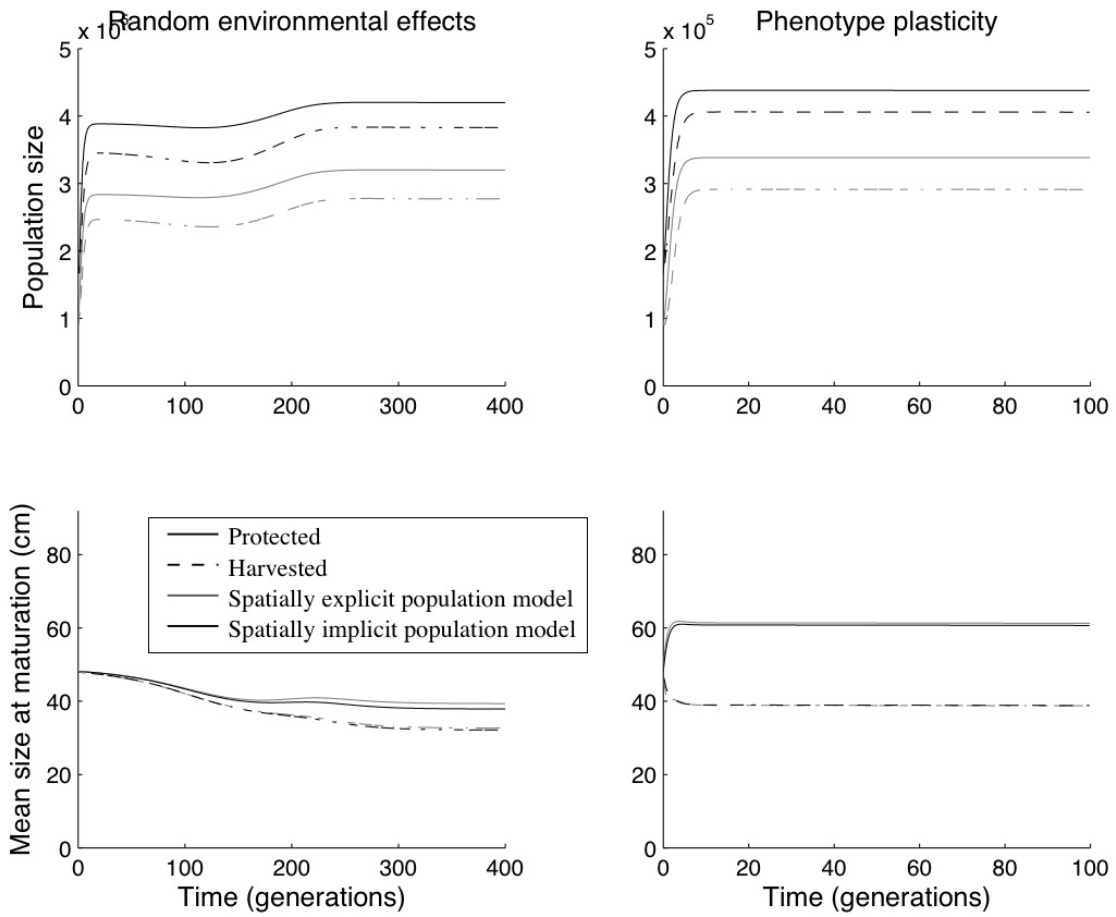


Figure D.1: Time trajectories for population size and size at maturation for bocaccio using the spatially explicit and spatially implicit models and the random environmental effects ( $\rho_f = 0$ ) and intermediate phenotype plasticity ( $\rho_f = 1 - h^2$ ) approaches, with long-distance dispersal ( $\sigma = 0.2$ ), one no-take reserve that covers 50% of the region, and a harvest mortality of 0.4 with a minimum size limit of 48 cm outside the protected area.

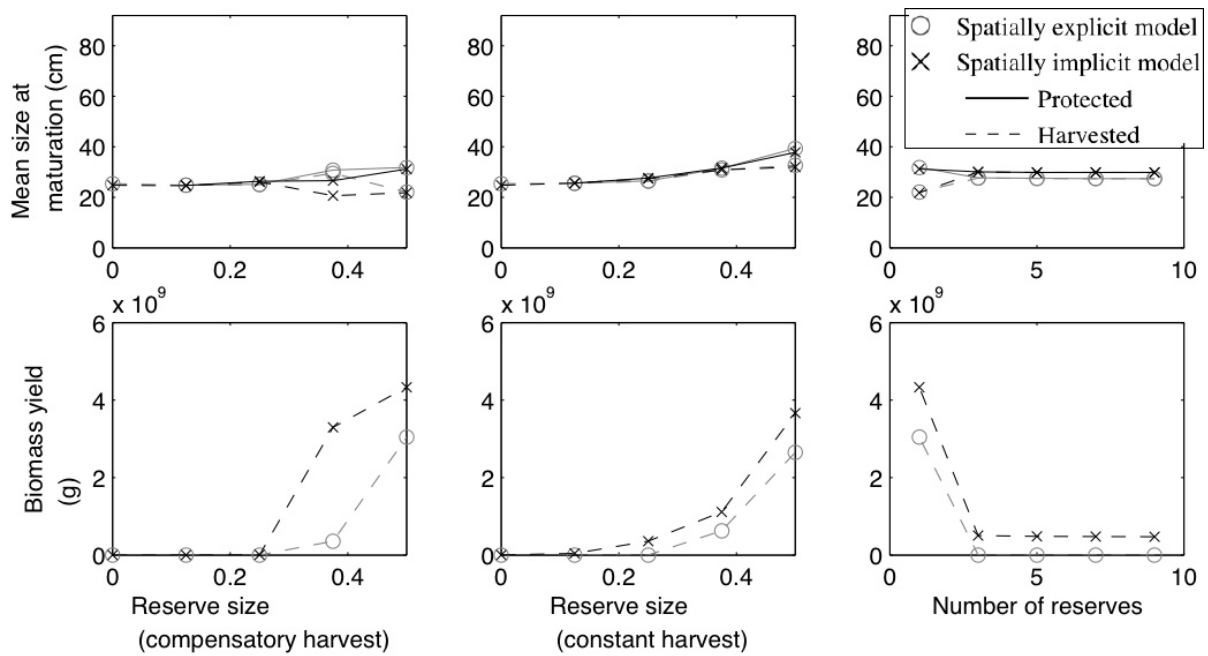


Figure D.2: Equilibrium mean size at maturation for the spatially explicit and spatially implicit models with random environmental effects, using parameters for bocaccio with long-distance dispersal ( $\sigma = 0.2$ ) and strong selection ( $h_H = 0.4$ , with minimum size limit  $S_m = 48$ ) outside the no-take MPA(s).

## E Details of the numerical simulation

The numerical simulation, programmed in *Matlab*, uses Runge-Kutta integration through time of equations (8)-(12) for the spatially implicit model (and, using Forward Time Centered Space integration, of (D.4)-(D.5) for the spatially explicit model) until each system reaches equilibrium. To numerically analyze the double integral in equations (12) or (D.5), we use a method involving Fourier Transforms developed by Turelli and Barton (1994). Let

$$y(g_1, g_2) = \psi^*(g_1)\psi^*(g_2) \quad (\text{E.1})$$

$$z(g_1, g_2) = \frac{1}{\sqrt{2\pi(G/2 + M)}} \exp\left[\frac{-\left(\frac{g_1+g_2}{2}\right)^2}{2(G/2 + M)}\right], \quad (\text{E.2})$$

where  $\psi^*(g)$  is defined as in equations (13) and (D.6). Then the convolution of the above functions is

$$c(g_1, g_2) = y * * z = \iint y(G_1, G_2)z(g_1 - G_1, g_2 - G_2)dG_1 dG_2, \quad (\text{E.3})$$

and the double integral in equations (12) and (D.5) is  $c(g, g)$ . By the Convolution Theorem of Fourier Transforms, the double integral becomes

$$c(g_1, g_2) = IFT[FT(c(g_1, g_2))] = IFT[FT(y(g_1, g_2))FT(z(g_1, g_2))], \quad (\text{E.4})$$

evaluated at  $g_1 = g_2$ . The fast Fourier Transform algorithm allows for rapid numerical calculation of equation (E.4).

## Literature Cited

MATLAB Version 6.5.0.1951 Release 13 2002.

Turelli, M. and Barton, N. H. 1994. Genetic and statistical-analyses of strong selection on polygenic traits: What, me normal? *Genetics* **138**:913–941.